UNIVERZITA PALACKÉHO V OLOMOUCI

Přírodovědecká fakulta

Katedra biochemie

Oxidační radikálové reakce v ultra-slabé emisi fotonů z kožních buněk

BAKALÁŘSKÁ PRÁCE

Autor:	**Anastasiia Balukova**
Studijní program:	B1406 Biochemie
Studijní obor:	Biotechnologie a genové inženýrství
Forma studia:	Prezenční
Vedoucí práce:	**M.Sc Ankush Prasad, Ph.D.**
Rok:	2018

PALACKY UNIVERSITY IN OLOMOUC

Faculty of Science

Department of Biochemistry

Involvement of oxidative radical reactions in ultra-weak photon emission from skin cells

BACHELOR THESIS

Author:	**Anastasiia Balukova**
Study programme:	B1406 Biochemistry
Branch of study:	Biotechnology and Gene Engineering
Form:	Full-time
Supervisor:	**M.Sc Ankush Prasad, Ph.D.**
Year:	2018

Prohlašuji, že jsem bakalářskou práci vypracovala samostatně s vyznačením všech použitých pramenů a spoluautorství. Souhlasím se zveřejněním bakalářské práce podle zákona č. 111/1998 Sb., o vysokých školách, ve znění pozdějších předpisů. Byla jsem seznámena s tím, že se na moji práci vztahují práva a povinnosti vyplývající ze zákona č. 121/2000 Sb., ve znění pozdějších předpisů.

V Olomouci dne …… ……..……..

I declare that I developed this bachelor thesis separately by showing all the sources and authorship. I agree with the publication of the thesis by Act no. 111/1998 Coll., about universities, as amended. I was aware of that the rights and obligations arising from the Act no. 121/2000 Coll., the Copyright Act, as amended, are applied to my work.

In Olomouc …… ……..…….

Acknowledgements

I would like to thank the supervisor of my thesis, M.Sc Ankush Prasad, PhD, for his kind help and patience, for giving me inspiration and valuable advice, and for his technical help and support when I was conducting the experiments and interpreting the results. I am also grateful to Doc. RNDr. Pavel Pospíšil, PhD and all the members of the Department of Biophysics, Centre of Region Haná for Biotechnological and Agricultural Research, Faculty of Science, Palacký University, Olomouc. Furthermore, I would like to thank my family and friends who encouraged me the whole way through my years of studies.

This work was financially supported by Student Grant Competition, grant no. IGA_PrF_2018_022 entitled "Modern Biophysics: New Directions and Perspectives".

Bibliografická identifikace

Jméno a příjmení autora	Anastasiia Balukova
Název práce	Oxidační radikálové reakce v ultra-slabé emisi fotonů z kožních buněk
Typ práce	Bakalářská
Pracoviště	Katedra biofyziky
Konzultant	Doc. RNDr. Pavel Pospíšil, PhD
Vedoucí práce	M.Sc Ankush Prasad, Ph.D.
Rok obhajoby práce	2018

Abstrakt

Kůže je trvale vystavena agresivním účinkům životního prostředí, například, biologickým, fyzikálním, chemickým atd. Reaktivní formy kyslíku (ROS) se vytváří během běžného metabolismu a jejich produkce se zvyšuje za stresových podmínek až na smrtelnou úroveň, což způsobuje oxidační stres. Peroxidace lipidů je dobře známým mechanismem buněčného poškození a často se používá jako indikátor oxidativního stresu v buňkách a tkáních. V současné studii byla pro studium v *ex-vivo* / *in-vitro* podminkách použita prasečí kůže, která je používána jako model pro lidskou kůži. V této práci jsou prezentovány experimentální výsledky týkající se zapojení hydroxylového radikálu ($HO^{\bullet}$) v lipidové peroxidaci a tvorbě elektricky excitovaných druhů, které nakonec vedou k ultra-slabým emisím fotonů. Při měření byly použity vychytávače singletového kyslíku ($^1O_2$) a také interferenční filter pro důkaz přítomnosti různých elektricky excitovaných druhů v celkové ultra-slabé emisi fotonů. Na základě získaných výsledků se ukázalo, že během oxidačních radikálových reakcí je ultra-slabá emise fotonů způsobena tvorbou jak tripletových excitovaných karbonylů ($^3L=O^*$), tak i $^1O_2$. Ultra-slabá emise fotonů může být použita jako vhodný neinvazivní nástroj pro sledování a vizualizaci oxidativních radikálových reakcí v kůži.

Klíčová slova	Singletový kyslík; tripletní excitovaný karbonyl; ultra-slabá emise fotonů; dvourozměrné zobrazení fotonů; kůže.
Počet stran	35
Počet příloh	01
Jazyk	Anglický

Bibliographical identification

Autor's first name and surname	Anastasiia Balukova
Title	Involvement of oxidative radical reactions in ultra-weak photon emission from skin cells
Type of thesis	Bachelor
Department	Department of Biophysics
Consultant	Doc. RNDr. Pavel Pospíšil, PhD
Supervisor	M.Sc Ankush Prasad, Ph.D.
The year of presentation	2018

Abstract

The skin is consistently exposed to environmental aggressions including biological, physical, chemical etc. Reactive oxygen species (ROS) are known to be formed during the normal metabolism which enhances to a lethal level under stress condition referred to as oxidative stress. Lipid peroxidation is a well-understood mechanism of cellular injury and is often used as an indicator of oxidative stress in cells and tissues. In the current study, we have used the porcine skin (intact pig ear/skin biopsies) as an *ex-vivo/in-vitro* model system to represent human skin. Experimental results showing the involvement of hydroxyl radical ($HO^{\bullet}$) in lipid peroxidation and the formation of electronically excited species eventually leading to ultra-weak photon emission are presented. To demonstrate the contribution of different electronically excited species in the overall ultra-weak photon emission, the effect of a scavenger of singlet oxygen ($^1O_2$) and measurement with interference filter on photon emission were measured. Based on the results obtained, it is concluded that during the oxidative radical reactions, the ultra-weak photon emission is contributed by the formation of both triplet excited carbonyls ($^3L=O^*$) and $^1O_2$. Ultra-weak photon emission is claimed to be an appropriate non-invasive tool for monitoring and visualization of oxidative radical reaction in the skin.

Keywords	Singlet oxygen; triplet excited carbonyl; ultra-weak photon emission; two dimensional photon imaging; skin.
Number of pages	35
Number of appendices	01
Language	English

Contents

Aims of Bachelor thesis

- To study the effect of reactive oxygen species (ROS) on ultra-weak photon emission
- Two-dimensional imaging of ultra-weak photon emission during oxidative radical reactions
- To demonstrate the involvement of electronically excited species in ultra-weak photon emission
- Understand the mechanism of oxidative damage to biomolecules

1 Introduction

The skin is the largest organ of the body and plays several essential functions such as thermoregulation, sensation, metabolism, and excretion (Morrow and Lechler, 2015). It acts as an external barrier, which protects the organisms from aggressions such as fluctuations in temperature, irradiations, toxic chemicals, etc. It is well known to be involved in the regulation of body temperature. Skin layers consist of the epidermis (the outermost layer) followed by dermis and hypodermis (also known as subcutis) which is the deepest layer (Chartier *et al*., 2017, Prost-Squarcioni, 2006, Meyer *et al*., 1994).

The epidermis is predominantly made up of dead cells (also known as corneocytes) that are firmly stuck together. The epidermis constantly renews itself within few weeks and new cells are made in the lower layers of the epidermis (Rinnerthaler *et al*., 2015). Under the epidermis lies the middle layer of skin (the dermis), which comprises extracellular molecules secreted by support cells. The dermal cells provide structural and biochemical support to the surrounding cells and consist of a dense network of tough elastic collagen fibres and bundles of elastin found in the extracellular matrix which makes the skin strong, robust and stretchy (Tepole *et al*., 2012). The hypodermis (also referred as subcutis) is mostly made up of fat and connective tissue (Fig. 1). The subcutis consists of tiny cavities which are filled with storage tissue made out of fat and water. It also stores metabolic products such as hormones, which are among the key components in the regulation of body functions.

The skin expresses receptors for peptide hormones and neurotransmitters, which are mostly aligned on the cell surface, and those for steroid and thyroid hormones, which are found in the cytoplasm or nuclear compartments (Zouboulis, 2009). The fat acts as a shock absorber, protecting bones and joints. Under the effect of any kind of abiotic stress (toxic chemicals, exposure to ultraviolet irradiations etc.), the epidermal and dermal cells are known to be most affected (Rinnerthaler *et al*., 2015, Ji and Li, 2016).

2 Current state of the topic

2.1 Porcine skin as a model system

Due to ethical reasons and difficulties pertaining to methodological aspects, human skins are generally replaced by an animal model system for *in-vivo* experimental research (Hikima *et al*., 2012, Abdullahi *et al*., 2014). At the same time, it also makes the experimentation cost-effective. Therefore researchers use animal models and *in-vitro* systems for skin experimentation to circumvent these difficulties. Effects of mechanical injuries/wounding or testing of a wide variety of new agents in experimental animals are possible but would be unjustifiable in humans. Thus, skin derived from animals has been extensively investigated to establish a suitable experimental model. The selection of the model system may depend on factors such as its availability, ease of handling, functional and anatomical similarity to that of humans. On a larger scale prevalent for testing of new agents/cosmetics etc. such as in cosmetic industries, small mammals are very often used; however, they differ from humans in anatomical and physiological ways (Kong and Bhargava, 2011).

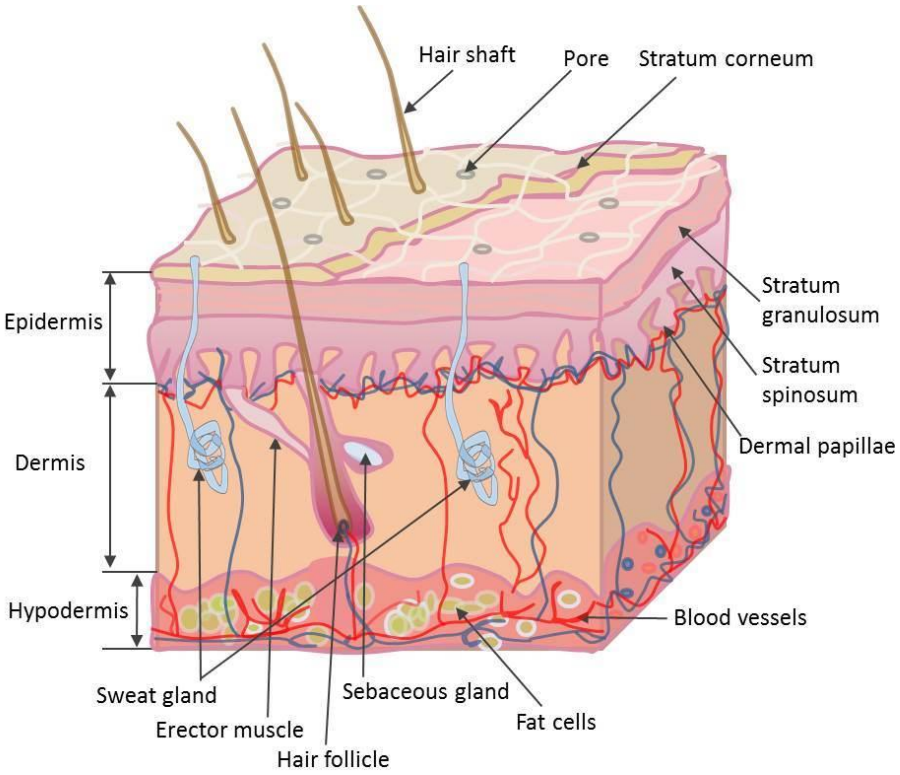

Figure 1: Schematic illustration of different components of human skin.

A multitude of morphologic, anatomic, immunohistochemical and dermatologic studies have demonstrated that porcine skin bears a strong similarity to human skin with respect to its morphology, cellular composition, and immunoreactivity (Avon and Wood, 2005). One of the striking similarity between porcine and human skin lies in the thickness of the epidermal layer (Jacobi *et al*., 2007). The epidermis of the porcine skin varies in thickness from 30 to 100 µm/70 to 140 µm, thus being within a range similar to human skin which is known to be in the range of 10 to 120 µm (Avon and Wood, 2005, Morris and Hopewell, 1990, Meyer *et al*., 1978). The enzymes of porcine epidermis also correspond in its overall histochemical profile to that of human skin; lipids contents in both cases comprises mainly of triglycerides and free fatty acids. The keratinous proteins of porcine and human skin are also known to be similar. While similarities between the porcine skin and human skin are numerous, differences are seen with respect to micro-morphology and function. Nevertheless, the porcine skin seems to be the most suitable model; having an epidermis and dermis that can be used as a model as there are clear structural, functional and biochemical characteristics comparable to human skin. Based on the above consideration, porcine skin is considered to be the most appropriate model, from the perspective of dermatological investigation among all other experimental models available.

2.2 Oxidative stress and ultra-weak photon emission

Oxidative stress occurs due to an imbalance between the production of reactive oxygen species (ROS) and a biological system's ability to detoxify the ROS/reactive intermediates. Oxidative stress may cause vital damage in cells and are known to be closely related with the development of several diseases including neurodegenerative diseases, ageing, cancers etc.. Measuring oxidative stress in the cell requires delicate assays. During the last few decades, oxidative metabolic reactions have been reported as a determinant of pathogenicity and thus, the introduction of a simple tool that can provide an information of the physiological state of the organism is a need of the time. Ultra-weak photon emission (UPE) which is also referred as biophoton emission/ low-level chemiluminescence has been proposed as a potential tool for measuring oxidative processes due to its association with ROS and overall, being able to serve as a non-invasive tool. Ultra-weak photon emission are well known to originate from the

relaxation of electronically excited species formed during the oxidative metabolic processes. The measurement of ultra-weak photon emission, however, remains challenging due to interference by stray photons and due to noise within the measurement system which might contribute to artefacts. For the purpose, isolation of the measurement system in dark are adopted and the detection device is cooled down to avoid thermal noise in the measurement (described in the next section).

Ultra-weak photon emission detection techniques are now extensively used to study the stress conditions pertaining to an oxidative radical reaction in the different living system (Kobayashi, 2005, Cifra and Pospisil, 2014, Poplova *et al*., 2017, Ou-Yang, 2014). Different range of living systems such as keratinocytes, fibroblast, skin homogenate, *ex-vivo* skin tissues as well as malignant skin cells have been measured *in-vitro* (Niggli *et al*., 2008, Torinuki and Miura, 1981, Madl *et al*., 2017). Spontaneous and stress-induced ultra-weak photon emission under exogenous exposure to stress factors such as irradiations (ultra-violet), smoke and toxic chemicals have also been documented in human skin, animals cells model and has been well summarized in recent reviews (Ou-Yang, 2014, Sauermann *et al*., 1999).

The involvement of ROS in ultra-weak photon emission has been experimentally presented in several studies. It has been claimed to occur via the oxidation of biomolecules (lipids, proteins and nucleic acid) (Pospíšil *et al*., 2014, Prasad and Pospisil, 2011a, Prasad and Pospisil, 2011c, Prasad and Pospisil, 2012, Prasad and Pospisil, 2013b, Poplova *et al*., 2017, Rastogi and Pospisil, 2011). Clinically, iron released by hemoglobin may be involved in the initiation of free radical chain reactions and can lead to ROS overproduction followed by peroxidation of lipids (Sadrzadeh *et al*., 1984, Rifkind *et al*., 2015). As a result of iron-induced Fenton's reaction or other transition metal ions, hydroxyl radicals ($HO^{\bullet}$) are known to be generated, which is known to be among highly reactive and short-lived ROS. The iron in the free form advocates the conversion of lipid hydroperoxides (LOOH) to lipid alcoxyl ($LO^{\bullet}$) radicals, which may reinitiate the lipid peroxidation process leading to enhanced oxidative damage.

In the current study, the induced ultra-weak photon emission was measured under the exogenous application of Fenton’s reagent generated chemically and applied topically on the skin before the start of photon emission measurement. The

electronically excited species which can be generated as a product of the oxidative radical reaction were investigated and their participation in the ultra-weak photon emission has been presented.

2.3 Ultra-weak photon emission and its detection

Ultra-weak photon emissions were detected using low noise photomultiplier tube (PMT) (for kinetic study) or using a highly sensitive charged couple device (CCD) camera (to generate a two-dimensional image). Researchers have used PMT/CCD cameras to measure ultra-weak photon emission from plants, animals and humans. However, since the flux of these photons are orders lower below the threshold for detection by human eyes or commonly used PMT/CCD systems, small fluctuation occurring in the living system is hardly recognizable. Thus, for the current purpose, higher sensitivity and low background (dark counts) is desirable (please refer to next section for details)

2.3.1 Photomultiplier tube (PMT)

The measurement of photons using PMT is based on Photoelectric effect, also known as photoemission, is a phenomenon in which electrically charged particles are released from or within a material when it absorbs electromagnetic radiation. The radiant energy may be from infrared till the gamma rays.

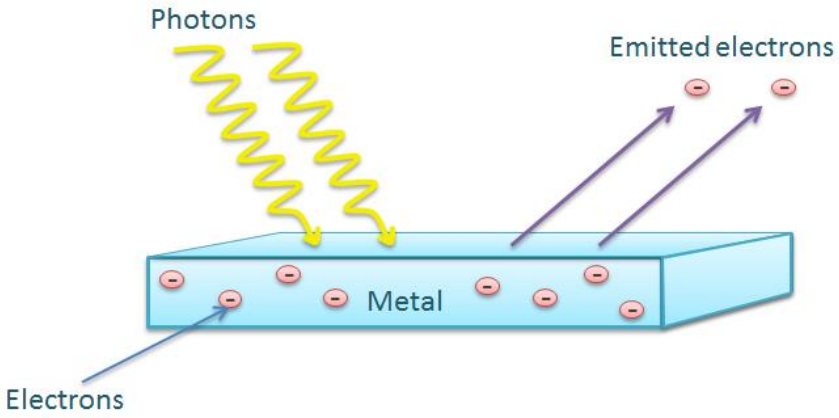

Figure 2: Schematic representation of Photoelectric effect

A schematic diagram of PMT components and its working principle is shown in Fig. 3. The window of a PMT is usually screened by a transparent shield to allow the photons to enter. Behind the shield lies a photocathode, in which the photon interacts with its material, emitting an electron by the photoelectric effect. The emitted electron/s are focused by focusing electrodes and accelerated to an array of dynodes which are connected by a chain of resistors giving each dynode more positive potential compared to the previous one. Because of the rising potential of the dynodes, more secondary electrons are emitted until they reach the anode with the maximal potential. On the anode, a voltage that is proportional to the initial number of photoelectrons is measured (Fig. 3).

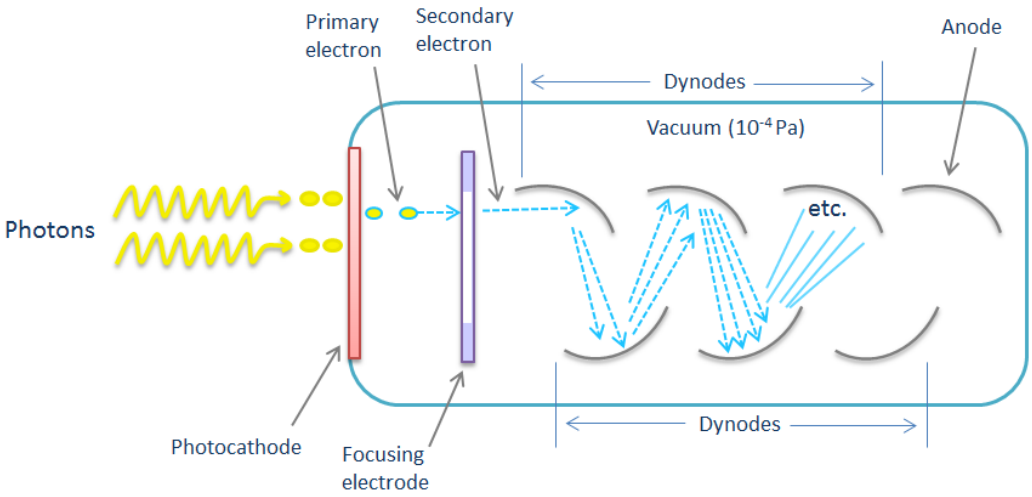

Figure 3: Schematic on the working principle of PMT.

2.3.2 Charge-coupled device (CCD)

Charge-coupled device image sensors are widely utilized in professional, medical application, and scientific research where high-quality images data are desirable. A CCD is a highly sensitive photon detector divided up into a large number of light-sensitive areas referred as pixels. These pixels are used to build up an image of the region of interest (ROI). When a photon falls within the area defined by one of the pixels, it is converted into one (or more) electrons and the numbers of electrons are directly proportional to the intensity at the said pixel. As the photons fall onto the CCD, the potential well attracts more electrons until the point where the potential well is full. The amount of electrons that can be accommodated under a pixel is known as the full well capacity. The final process on the CCD chip is reading of each pixel so that the associated charge can finally be measured. At the end of the readout register lies an amplifier which measures the value of each charge and converts finally into a voltage. The pixels value are then digitized and the output value of each pixel is processed using the interface, where the image is processed and displayed.

Thermal generation of electrons can occur and are indistinguishable from photo-generated electrons. This constitutes a noise source commonly referred as dark current and it is highly important to reduce their number to avoid any interference in measurement. The removal of the noise components achieved using low temperature and removal of background noise plays a key role in acquiring two-dimensional ultra-weak photon emission images. The measurement conditions are explained in the follow-up sections.

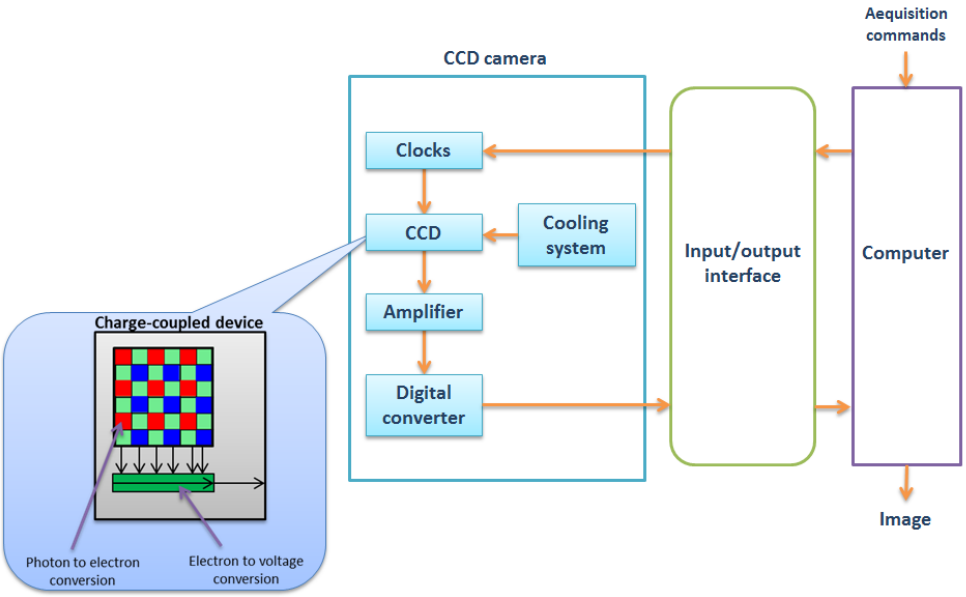

Figure 4: Schematic representation on the working of CCD camera

3 Materials and methods

3.1 Porcine ear/skin biopsy

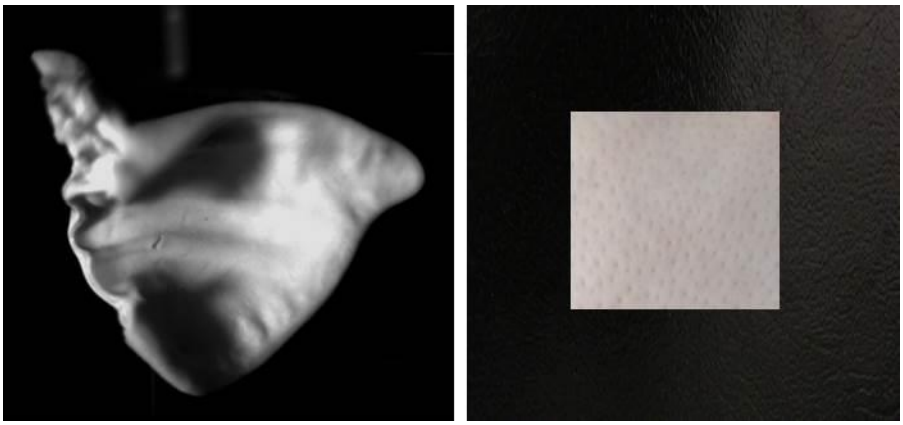

Figure 5: Photograph of porcine ear (left panel) taken using CCD camera (VersArray 1300B (Princeton Instruments, Trenton, NJ, USA) and skin biopsy (right panel).

Intact pig ears were obtained from a local slaughterhouse in Olomouc, Czech Republic and transported to the laboratory at low-temperature (in ice box). The skin biopsies were prepared as per the procedure described with minor modifications (Chiu and Burd, 2005). Fresh skin samples collected each day were used during the tenure of study.

3.2 Chemicals

Fenton's reagent was prepared using a solution of hydrogen peroxide (H_2O_2) (Sigma-Aldrich Chemie GmbH, Germany) and ferrous sulfate ($FeSO_4.7H_2O$) (BDH Laboratory Supplies, UK). In all experiments, a fixed concentration of $FeSO_4$ (500 µM) and a variable concentration of H_2O_2 (either 100 µM or 1 mM) was used. Spin trap, POBN [α-(4-Pyridyl 1-oxide)-N-tert-butylnitrone] was purchased from Sigma-Aldrich Chemie GmbH, Germany.

$$Fe^{2+} + H_2O_2 \rightarrow Fe^{3+} + HO\bullet + OH^-$$

Chemical reaction: Fenton's reaction showing the generation of a $HO^{\bullet}$ and a hydroxide ion formed from a solution of H_2O_2 with ferrous iron as a catalyst. Iron(II) is oxidized by H_2O_2 to iron(III).

3.3 EPR spin-trapping spectroscopy

Electron paramagnetic resonance (EPR) allows detection of ROS directly. It bears the unique ability to detect short-lived as well as long-lived radical species with high specificity and sensitivity. In our study, to confirm the formation of $HO^{\bullet}$ during the Fenton's reaction, EPR spectra of POBN-OH adduct was detected at 20 µM H_2O_2 in the presence of 100 µM $FeSO_4$ (Fig. 7). Hydroxyl radical was detected using 4-pyridyl-1-oxide-N-tert-butylnitrone (POBN) [25mM] spin-trapping system in a glass capillary tube (Blaubrand intraMARK, Brand, Germany). EPR spectra were recorded using an EPR spectrometer MiniScope MS400 (Magnettech GmbH, Berlin, Germany) with following EPR conditions: microwave power, 10 mW; modulation amplitude, 1 G; modulation frequency, 100 kHz; sweep width, 100 G; scan rate, 1.62 G s^{-1}, gain, 100.

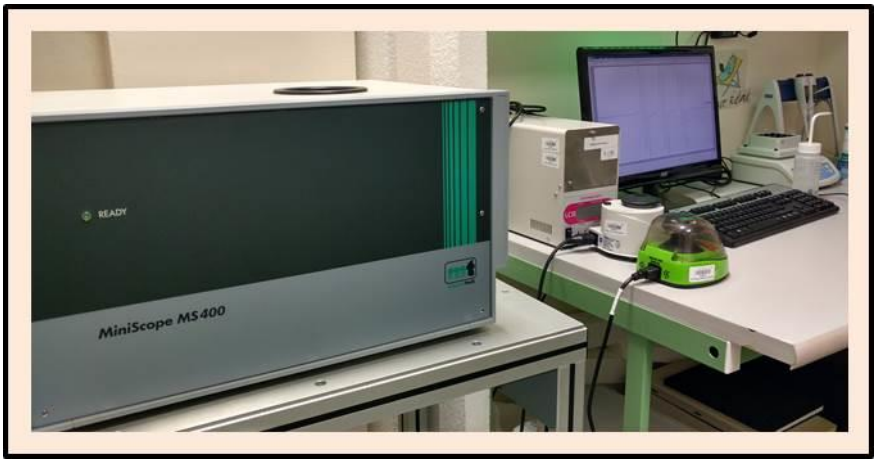

Figure 6. The EPR spectrometer MiniScope MS400 (Magnettech GmbH, Berlin, Germany) at the Department of Biophysics (CRH) that was used in the present study.

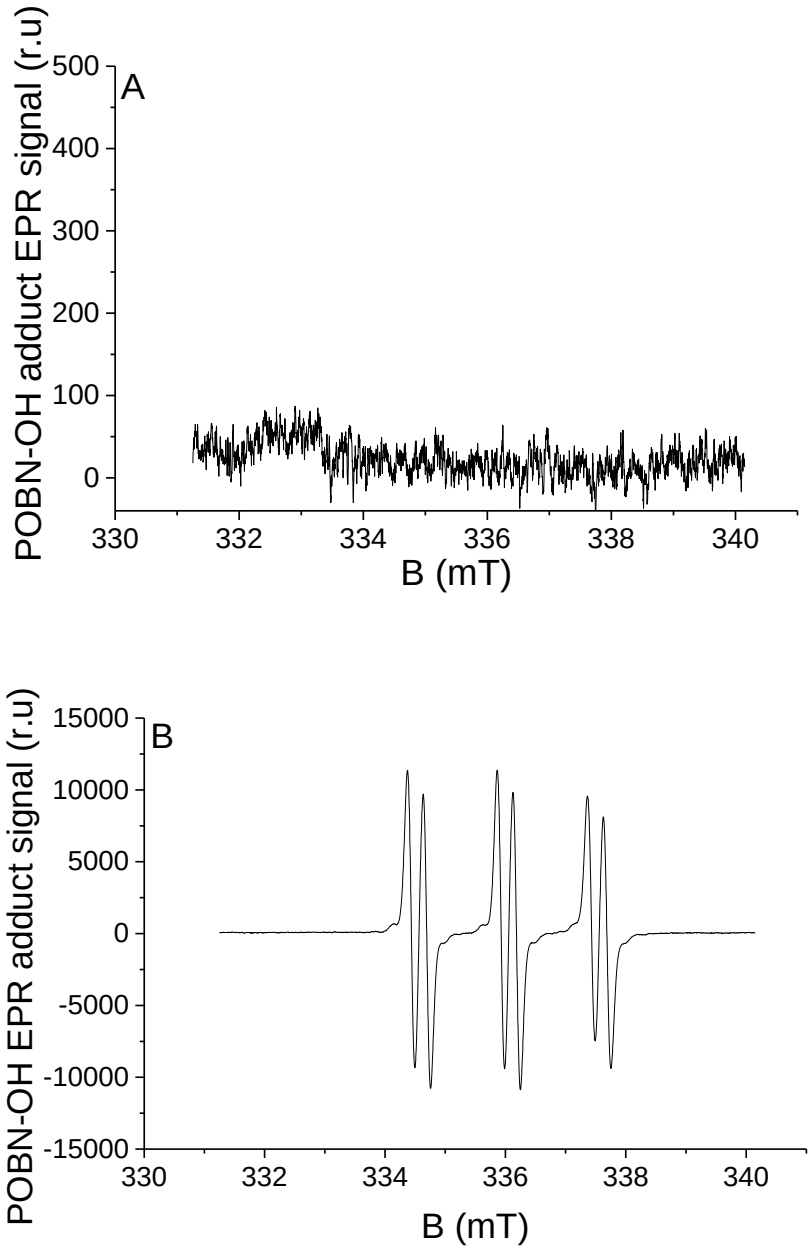

Figure 7: EPR spectra of POBN-OH adduct detected in solutions containing 100 µM $FeSO_4$ in the absence (a) and presence of 20 µM (b) of H_2O_2.

3.4 Measurement setup and experimental conditions

For the measurement of ultra-weak photon emission, it is a pre-requisite to specifically design a dark room to avoid any kind of interference from stray photons.

In our current study, ultra-weak photon emission measurements were done in an experimental dark room as described (Prasad and Pospisil, 2013a). A schematic representation of dark room and of measurement setup have been shown in Figs. 10

and 11. All experiments were done in replicates and the representative graph has been presented.

3.4.1 Fenton's reagent-induced kinetic measurement of ultra-weak photon emission

Fenton's reagent in the concentration of 500 µM $FeSO_4$ and 100 µM H_2O_2 or 1 mM H_2O_2 were topically applied to skin biopsies. The mentioned concentrations of Fenton's reagent were selected based on a thorough testing of different concentration and monitoring the change in ultra-weak photon emission. Fenton's reagent was topically applied after the start of measurements, usually within first few minutes (indicated by arrows in each case). Sodium ascorbate (Sigma-Aldrich Chemie GmbH, Germany) at a final concentration of 5 mM was added 20 s prior to the topical application of Fenton's reagent.

3.4.2 Fenton's reagent-induced ultra-weak photon emission in the blue-green region of the spectrum

The spectral distribution of ultra-weak photons emitted during exogenous application of Fenton's reagent was studied using a blue-green interference filter type 644 (Schott & Gen., Jena, Germany) (Fig. 8). The transmission of the filter chosen was in the range 340-540 nm for reflecting the contribution of triplet carbonyls ($^3L=O^*$) in the photon emission. The filter was mounted in front of PMT window and the kinetics of ultra-weak photon emission was monitored from the porcine skin biopsies after the topical application of Fenton's reagent (1 mM H_2O_2 containing 500 µM $FeSO_4$).

Figure 8: Photograph of blue-green interference filter type 644.

3.5 Ultra-weak photon emission

3.5.1 Two-dimensional imaging of ultra-weak photon emission

Figure 9. The CCD camera VersArray 1300B (Princeton Instruments, Trenton, NJ, USA) at the Department of Biophysics (CRH) used in the present study.

Ultra-weak photon emission imaging was measured in porcine ear and skin biopsies using highly sensitive CCD camera. All samples were kept in dark for 30 min to avoid any interference by delayed luminescence (Prasad and Pospisil, 2011b). Other experimental conditions are as per the procedure outlined in listed references (Prasad *et al*., 2016, Prasad and Pospisil, 2011c). CCD camera VersArray 1300B (Princeton Instruments, Trenton, NJ, USA) with the spectral sensitivity of 350–1000 nm and almost 90% quantum efficiency in the visible range of the spectrum was used under following parameters: scan rate, 100 kHz; gain, 2; an accumulation time, 30 min/45 min (porcine ear/skin biopsies). CCD camera was cooled down to -104 °C using a liquid-nitrogen cooling system for reduction of dark current. Before each measurement, the data correction was made by subtracting the background noise.

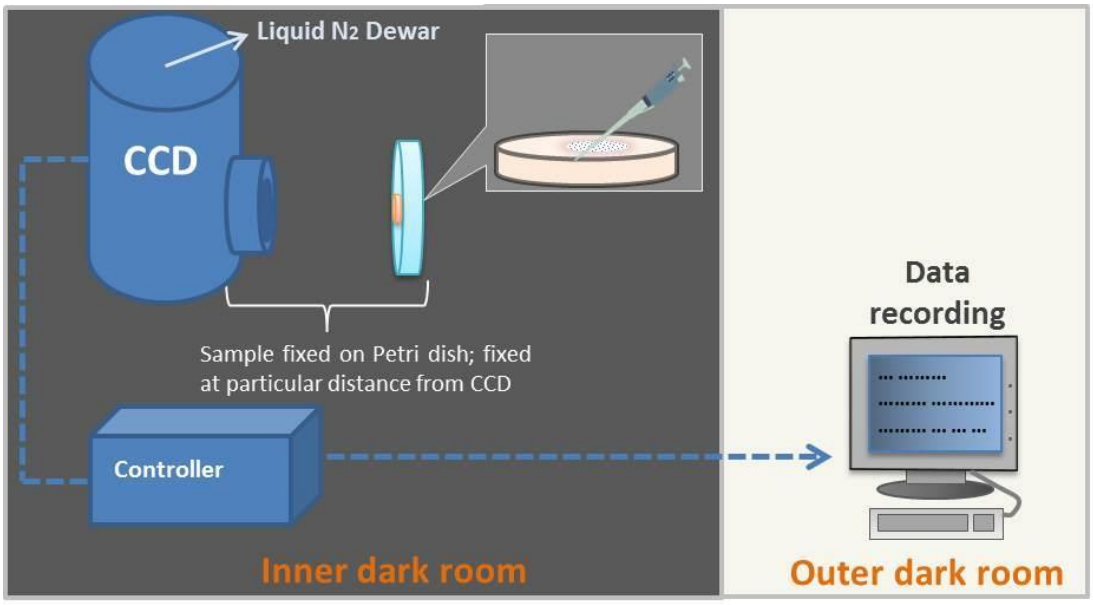

Figure 10: Schematic illustration of the experimental setup for detection of two-dimensional imaging of ultra-weak photon emission.

3.5.2 Kinetics of ultra-weak photon emission in the visible and near-infrared region of the spectrum

The kinetics of ultra-weak photon emission in the visible region of the spectrum was performed using PMT (type R7518P) [spectral sensitivity: 185-730 nm; detection area: Ø 28mm]. To reduce the thermal electrons, the PMT was cooled down to -30°C using thermoelectric cooler C9143 (Hamamatsu Photonics, K.K., Iwata City, Japan).

The kinetics of ultra-weak photon emission in the near-infrared region was measured using a high-speed near-infrared PMT (type H10330C-45) (Hamamatsu Photonics K.K., Iwata City, Japan) [spectral sensitivity: 950-1400 nm; detection area: Ø 18mm]. The photon counts in both cases were recorded using low-noise photon counting unit (C9744, Hamamatsu Photonics K.K., Iwata City, Japan).

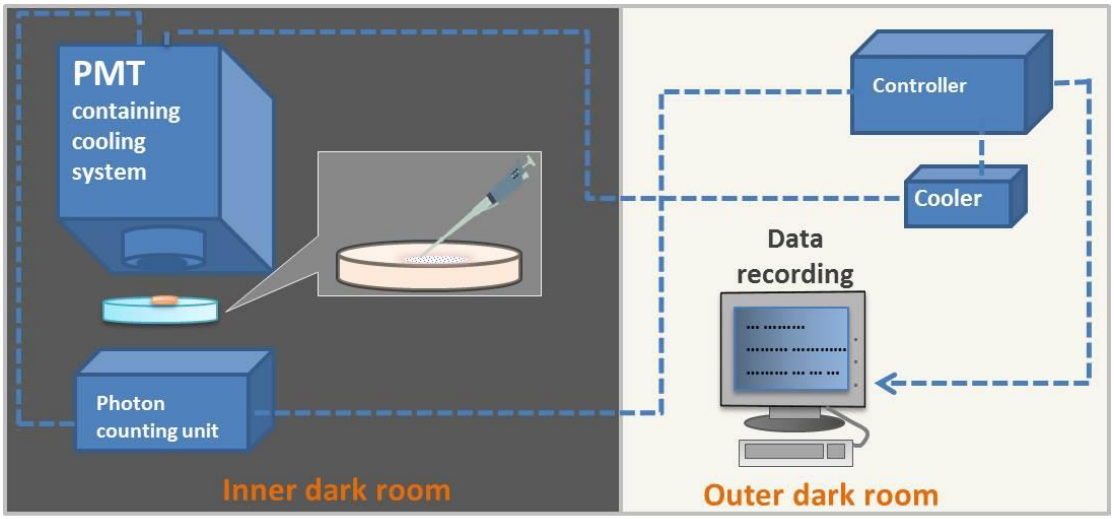

Figure 11: Schematic illustration of the experimental setup for detection of kinetic measurements of ultra-weak photon emission.

4 Results

4.1 Fenton's reagent-induced kinetic measurement of ultra-weak photon emission

Ultra-weak photon emission kinetics was measured following the topical application of Fenton's reagent from the porcine skin biopsies using visible PMT. Prior to the start of measurements, the dark count in the experimental dark room was monitored and recorded to be ~2 photon counts s^{-1} (Fig. 12A). Since, some chemical components are known to interfere with photon emission measurement, as additional controls, the photon emission from H_2O_2; Fenton's reagent and sodium ascorbate were measured separately/in combinations to test any kind of interference/contribution in overall ultra-weak photon emission. It was observed that the contribution of chemicals (in the absence of skin sample) showed signal intensity comparable to the photon count as observed in dark (Fig. 12 B-D).

With the exposure of skin biopsies to Fenton's reagent in the concentration of 500 µM $FeSO_4$ and 100 µM H_2O_2 (Fig. 13A) or 1 mM H_2O_2 (Fig. 13B), it can be observed that the ultra-weak photon emission was enhanced to ~80 counts s^{-1} and ~250 counts s^{-1}, respectively which then decayed over time. Based on this current observation, it can be concluded that the Fenton's reagent which acts as an oxidant for the biomolecules (described in the later section) contributes as a key factor for ROS-mediated ultra-weak photon emission. In the next set of experiments (as otherwise indicated), it was chosen 1 mM H_2O_2 containing 500 µM $FeSO_4$ as the inducer of ultra-weak photon emission. The above concentration was chosen since the photon emission is in the range of tens of photon counts s^{-1} and thus the effect of scavenger and interference filters used in the follow-up experiments would be visible.

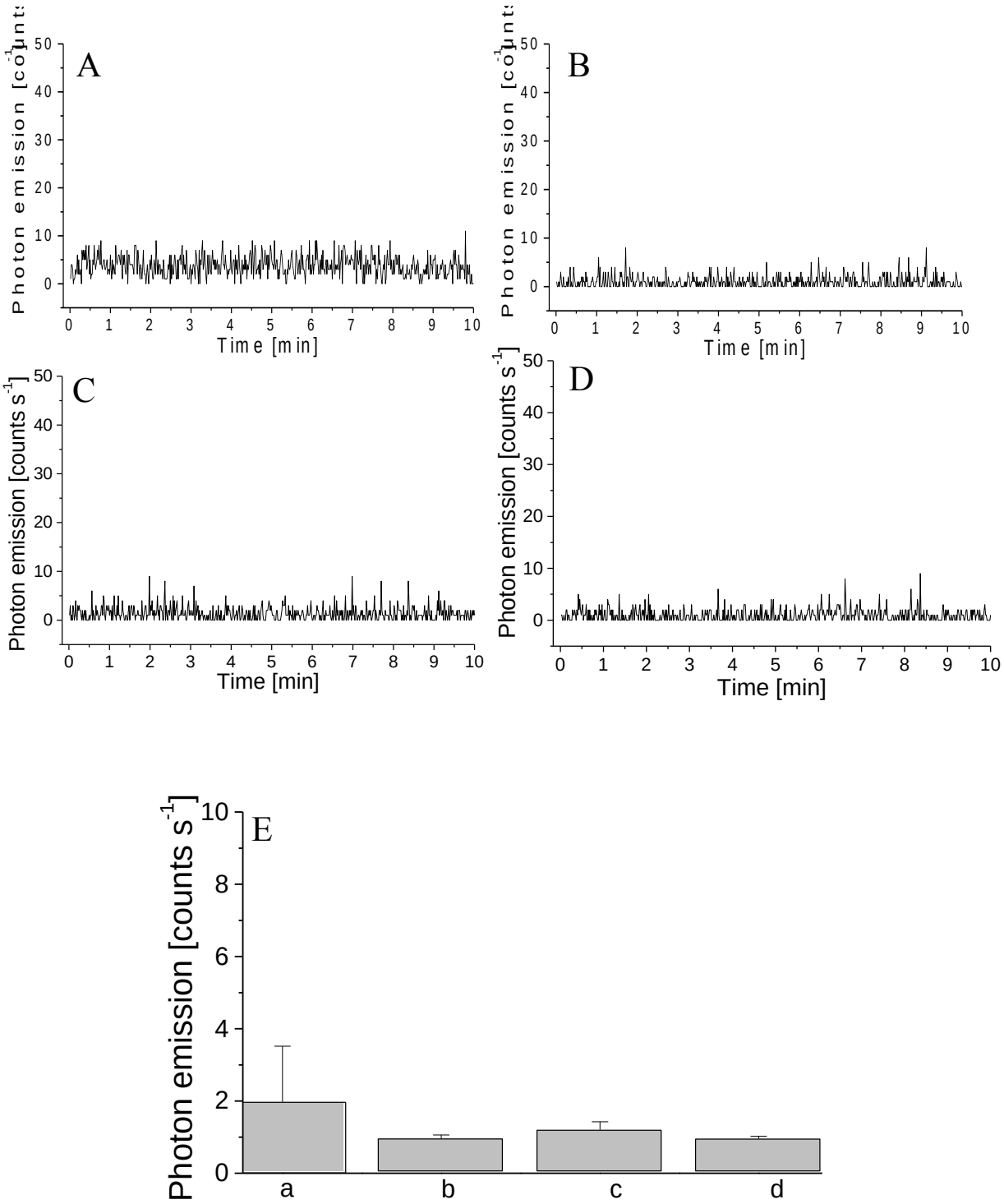

Figure 12: Ultra-weak photon emission measured using visible photomultiplier tube (PMT). Kinetics of ultra-weak photon emission was measured in dark (A); in the presence of Fenton's reagent (100 µM H_2O_2 containing 500 µM $FeSO_4$) (B); in the presence of Fenton's reagent (1 mM H_2O_2 containing 500 µM $FeSO_4$) and in the presence Fenton's reagent (1 mM H_2O_2 containing 500 µM $FeSO_4$) containing 5 mM sodium ascorbate. The decay curve was measured for a duration of 10 min. The presented data are expressed as mean value of photon emission and the standard deviation of at least three measurements (mean ± SD, n=3) (E).

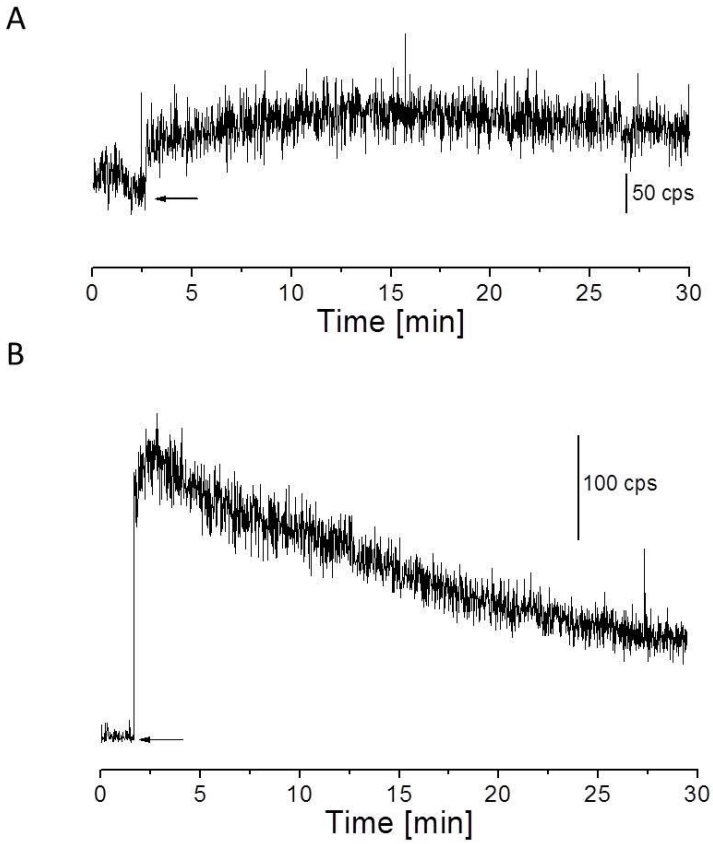

Figure 13: Kinetics of Fenton's reagent-induced ultra-weak photon emission measured using visible PMT from the porcine skin sample. Kinetics of ultra-weak photon emission was measured after the topical application of Fenton's reagent (100 µM and 1 mM, containing 500 µM $FeSO_4$), respectively added after ~2 min of the start of measurement (indicated by arrow). The decay curve was measured for duration of 30 min.

4.2 Fenton's reagent-induced ultra-weak photon emission in the blue-green region of the spectrum

The spectral distribution of ultra-weak photons emitted during the exogenous application of Fenton's reagent to skin biopsy was studied using an interference filter (type 644 with a transmission in the range 340–540 nm) (Fig. 14). The interference filter was mounted in the front of PMT window.

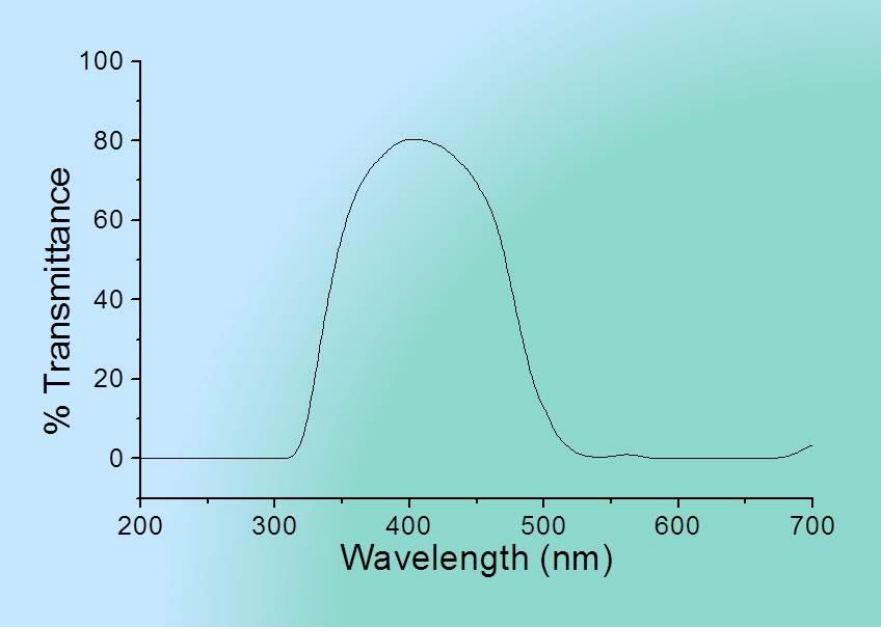

Figure 14: Transmission spectrum of interference filter type 644 (Schott & Gen., Jena, Germany)

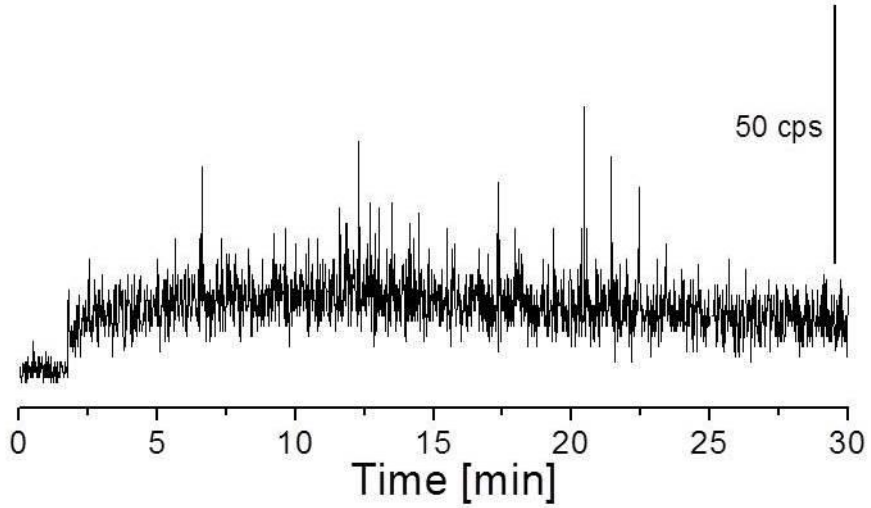

Figure 15: Kinetics of ultra-weak photon emission measured after the topical application of Fenton's reagent (containing 1 mM H_2O_2 and 500 µM $FeSO_4$) in the presence of interference filter type 644 (340–540 nm).

The kinetics of ultra-weak photon emission from the porcine skin biopsies was measured after the exogenous application of Fenton's reagent (1 mM H_2O_2 containing 500 µM $FeSO_4$). It can be seen that the application of Fenton's reagent enhanced the ultra-weak photon emission only to ~25 counts s^{-1} in contrary to 250 counts s^{-1} observed in the absence of interference filter (Figs. 15 and 13B). The observation provides a clear indication that not all ultra-weak photon emission observed in

Fenton’s reagent-induced process is a resultant of species emitting the blue-green region of the spectrum. It can be due to the involvement of other electronically excited species. Nevertheless, a small reduction in photon counts can be also contributed by % transmittance of the interference filter.

4.3 Fenton’s reagent-induced imaging of ultra-weak photon emission

Ultra-weak photon emission imaging was measured from the porcine ear and skin biopsies after the exogenous application of Fenton’s reagent using CCD camera (Figs. 16 and 17). Fig. 16 shows the photograph (left panel) and two-dimensional imaging of ultra-weak photon emission (right panel) from an *ex-vivo* porcine ear.

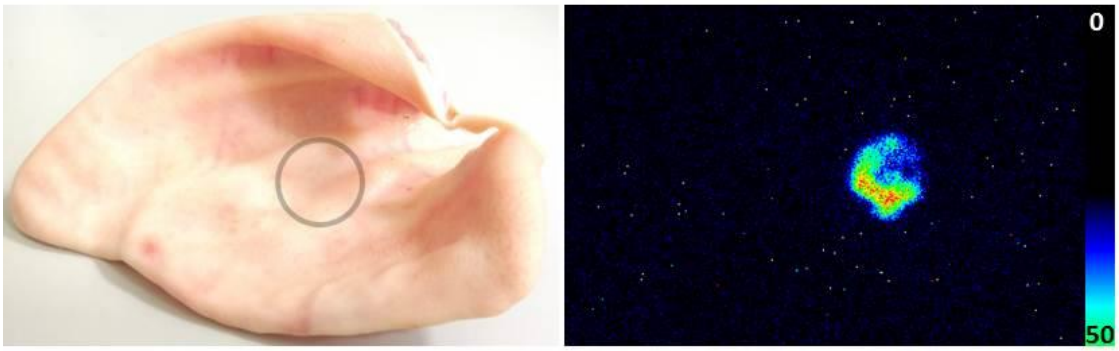

Figure 16: Two-dimensional Fenton’s reagent-induced ultra-weak photon emission measured using CCD camera from the porcine ear. A. Photograph of pig ear (circle represents the area of the porcine ear where Fenton’s reagent was topically applied) and two-dimensional ultra-weak photon emission imaging measured after the topical application of Fenton’s reagent (1 mM H_2O_2 containing 500 µM $FeSO_4$).

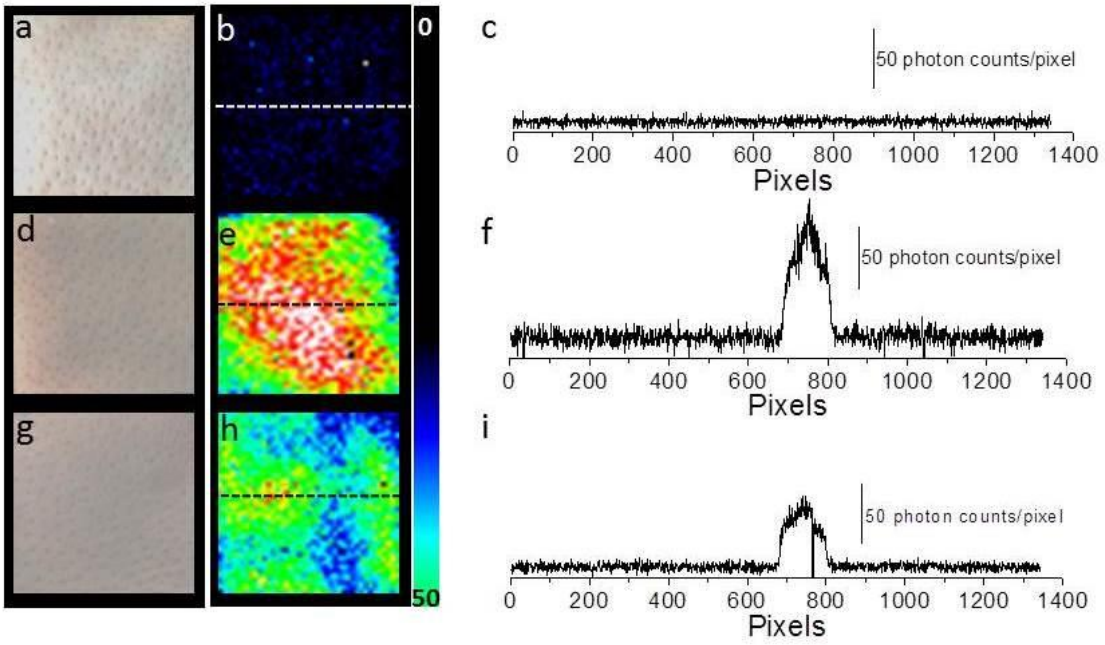

Figure 17: Left panel: Photographs (a, d and g) and corresponding two-dimensional images of ultra-weak photon emission of spontaneous (b), induced with Fenton's reagent (1 mM H_2O_2 containing 500 µM $FeSO_4$) (e) and induced with Fenton's reagent (1 mM H_2O_2 containing 500 µM $FeSO_4$ and sodium ascorbate) (5 mM) (h). Right panel: (c, f and i) shows the spatial profile of the photon emission in a single strip of the image (dashed line) in spontaneous (c), Fenton's reagent-induced (f) and Fenton's reagent-induced in the presence of sodium ascorbate (i). Y-axis reflects the number of photon counts accumulated after 30 min, whereas the X-axis denotes the pixel of the image.

In Fig. 16, two-dimensional imaging of ultra-weak photon emission was performed after the treatment with Fenton's reagent (1 mM H_2O_2) containing 500 µM $FeSO_4$. Fig. 17 shows the photograph (la, d and g), two-dimensional imaging of ultra-weak photon emission (b, e, and h) and intensity of ultra-weak photon emission (c, f and i) from skin biopsies. The ultra-weak photon emission imaging was measured in the absence (b) and presence of Fenton's reagent (e and h). In (e), Fenton's reagent was topically applied to skin biopsy and measured subsequently while in (h); sodium ascorbate (5 mM) which is a scavenger of singlet oxygen ($^1O_2$) was added immediately before the topical application of Fenton's reagent. It can be seen that the presence of sodium ascorbate prior to application of Fenton's reagent considerably suppressed the ultra-weak photon emission from the skin. As it can be observed from the intensity of ultra-weak photon emission, the skin which remains untreated with Fenton's reagent (c) does not show any increase while the skin treated

with exogenous application of Fenton's reagent (1 mM H_2O_2) containing 500 µM $FeSO_4$ shows an intensity maximum of ~150 counts/pixel. It was found to be suppressed by ~50% in case of skin biopsy pre-treated with sodium ascorbate. Based on this observation, it is quite clear that the participation of $^1O_2$ dimol photon emission in the total ultra-weak photon emission observed cannot be completely neglected. The above observation was further validated by monitoring the effect of sodium ascorbate on Fenton's reagent (1 mM H_2O_2) containing 500 µM $FeSO_4$ on skin biopsy. It was observed that the ultra-weak photon emission was suppressed by ~5 times in the presence of sodium ascorbate (Fig. 18).

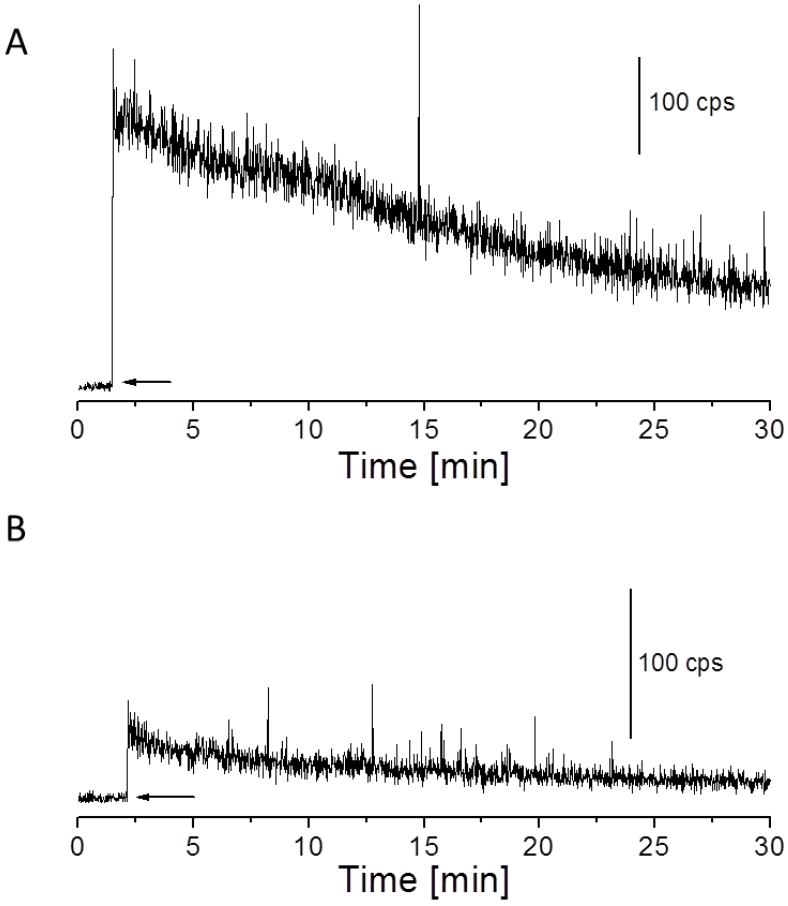

Figure 18: Kinetics of Fenton's reagent-induced ultra-weak photon emission measured using visible PMT from the porcine skin sample. In A, kinetics of ultra-weak photon emission was measured after the topical application of Fenton's reagent (containing 1 mM H_2O_2 and 500 µM $FeSO_4$). In B, sodium ascorbate (5 mM) was added prior to treatment with Fenton's reagent. Other experimental conditions as in Fig. 13

4.4 Fenton's reagent-induced ultra-weak photon emission in the near-infrared region of the spectrum

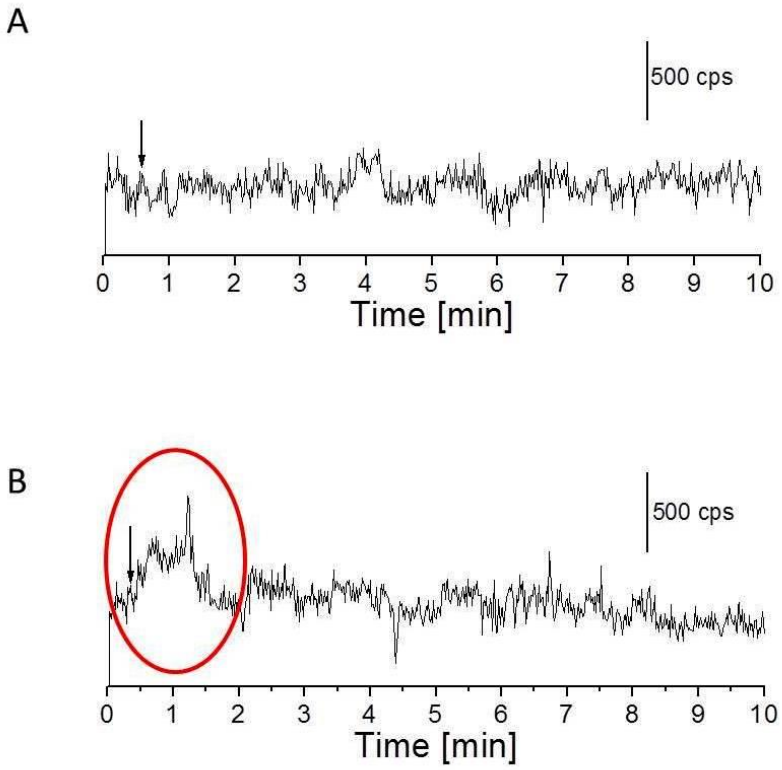

Figure 19: Kinetics of Fenton's reagent-induced ultra-weak photon emission measured using near-infrared PMT from the porcine skin sample. In A and B, kinetics of ultra-weak photon emission was measured after the topical application of Fenton reagent (100 µM and 1 mM, containing 500 µM $FeSO_4$), respectively. Fenton's reagent was added between 30 seconds to 1 min of the start of measurement (indicated by arrow) and the decay curve was measured for a duration of 10 min.

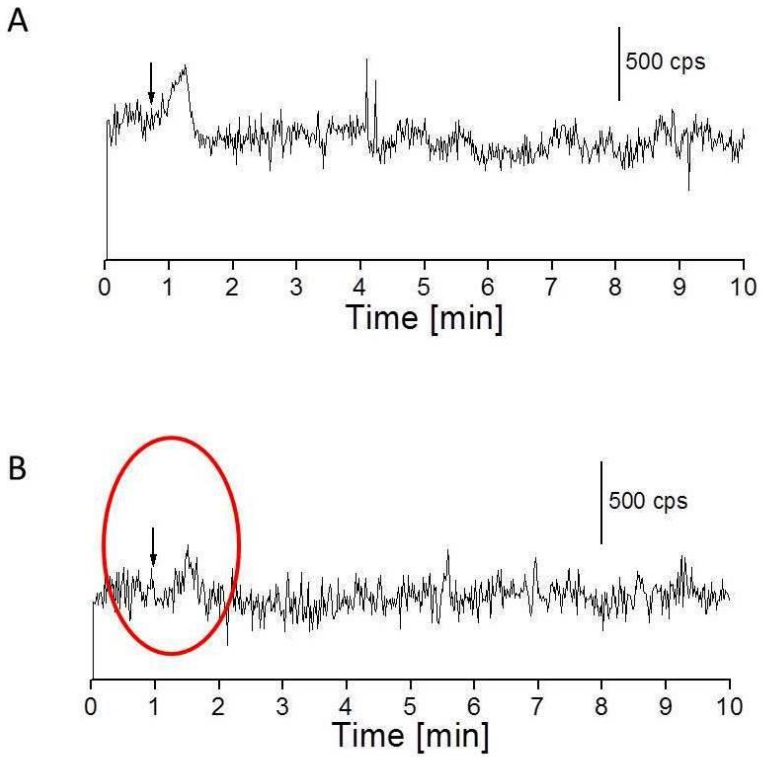

Figure 20: Kinetics of Fenton's reagent-induced ultra-weak photon emission measured using near-infrared PMT from the porcine skin sample. In A, kinetics of ultra-weak photon emission was measured after the topical application of Fenton's reagent (containing 1 mM H_2O_2 and 500 µM $FeSO_4$). In B, sodium ascorbate (5 mM) was added prior to treatment with Fenton's reagent. Other experimental conditions as in Fig. 19

To further understand and clarify the participation and contribution of different electronically excited species, kinetics of ultra-weak photons emitted during the oxidative radical process mediated by Fenton's reagent was measured in the near-infrared region using a high-speed near-infrared PMT with a spectral sensitivity in the range of 950-1400 nm. The skin biopsy was topically applied with Fenton's reagent in the concentration of 100µM (A) H_2O_2 and 1 mM H_2O_2 (B) containing 500µM $FeSO_4$ (Fig. 19). It can be observed that with the application of lower concentration (100µM containing 500µM $FeSO_4$) of Fenton's reagent, no detectable enhancement in ultra-weak photon emission was observed while application of higher concentration (1mM containing 500µM $FeSO_4$) of Fenton's reagent enhanced the ultra-weak photon emission to about 800 counts s^{-1} which then decayed within 2 min (Fig. 19B). Using near-infrared PMT, Fenton's reagent-induced kinetics of ultra-weak photon emission was also measured in the presence of sodium ascorbate (Fig. 20). It can be clearly

seen that in the presence of sodium ascorbate, Fenton's reagent-induced ultra-weak photon emission was significantly suppressed as in agreement with results obtained in Fig. 17 (h and i) and Fig. 18.

5 Discussion

5.1 Oxidative radical reaction and triplet excited carbonyls

The oxidation of polyunsaturated fatty acid (PUFA) mediated by $HO^{\bullet}$ initiates with the abstraction of hydrogen from the hydrophobic tail of the lipid molecule (L) and results in the formation of an alkyl radical ($L^{\bullet}$). In the presence of molecular oxygen (O_2), it leads to the formation of lipid peroxyl radical ($LOO^{\bullet}$) (Halliwell and Gutteridge, 2007). The epidermal and the dermal layer of both the porcine or human skin contains a high percentage of PUFA and thus access to the lipid molecules and further oxidation is very likely. The formation of $LOO^{\bullet}$ and its further accumulation, the interaction with another $LOO^{\bullet}$ becomes very likely. The self-reaction of $LOO^{\bullet}$ leads to the formation of $^{3}(C=O)^{*}$ and molecular oxygen or the ground state of carbonyls (C=O) and $^{1}O_2$ via the formation of tetroxide (LOOOOL) (Fig. 21) (Russell, 1957, Miyamoto *et al*., 2014, Cadenas and Sies, 2000). Besides this, $LOO^{\bullet}$ can also react with neighbouring lipid molecule and can be involved in the formation of LOOOOL via the formation of reactive intermediates such as LOOH. Alternate to this pathways, cyclic high-energy intermediates dioxetanes (LOOL) can be generated by the cyclisation of $LOO^{\bullet}$ (Corey and Wang, 1994). As a result of oxidative metabolic processes, electronically excited species such as $^{3}L=O^{*}$ are formed by the decomposition of high-energy intermediates (LOOL and LOOOOL) (Fig. 21) (Cilento and Adam, 1995, Adam and Cilento, 1982). The decrease in Fenton's reagent-induced ultra-weak photon emission from the porcine skin in the presence of interference filter (in the blue-green region) was significant. It clearly shows that $^{3}L=O^{*}$ is one of the major participants in the overall ultra-weak photon emission (Fig. 15). The participation of $^{3}L=O^{*}$ in ultra-weak photon emission has been lately reported in several studies (Havaux, 2003, Footitt *et al*., 2016); however, the contribution of other molecules cannot be completely neglected. The decomposition of high-energy intermediates (LOOL and LOOOOL) leads to the generation of $^{3}L=O^{*}$ which can undergo an electronic transition from the triplet excited state to the ground state emitting ultra-weak photons in the varied region of the spectrum [near UVA and blue-green regions of the spectrum (350-550 nm)].

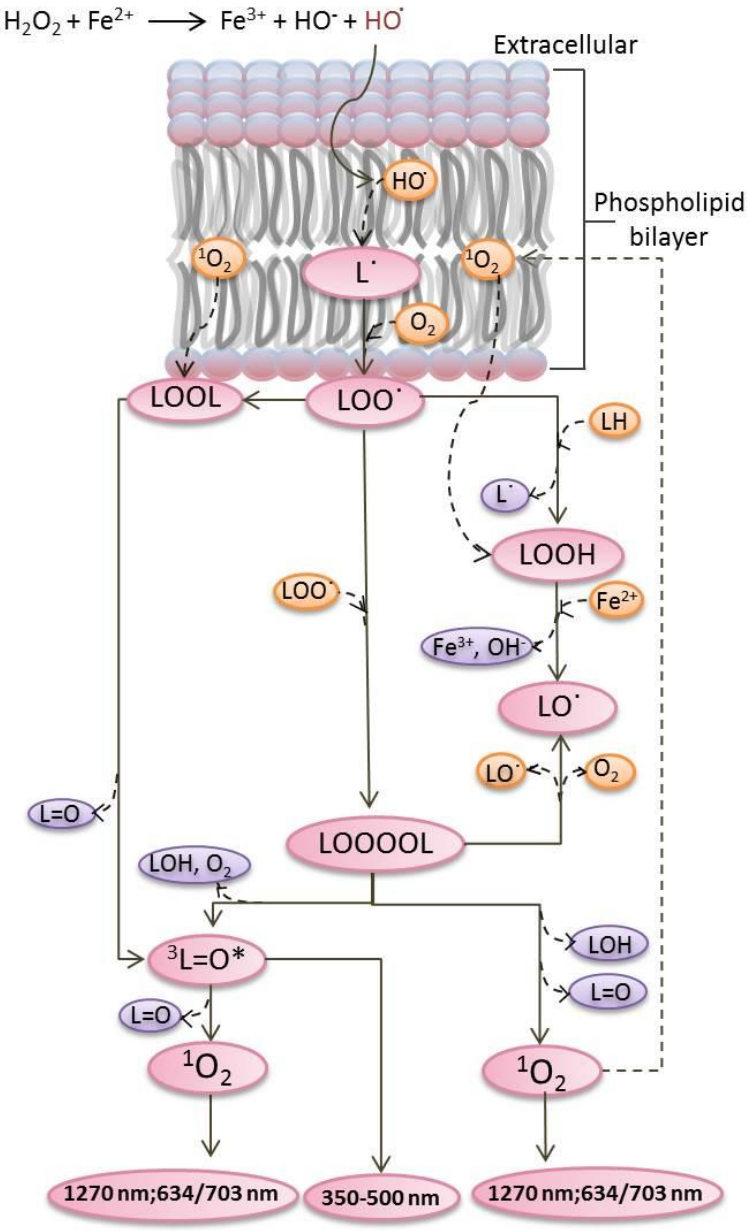

Figure 21: Mechanism of the formation of electronically excited species [triplet excited carbonyls ($^3C=O^*$) and singlet oxygen ($^1O_2$)] by oxidative metabolic processes via oxidation of polyunsaturated fatty acid initiated by Fenton's reagent.

5.2 Oxidative radical reaction and singlet oxygen

In an oxygenic environment, the excitation energy can be transferred from $^3L=O^*$ to O_2 via triplet-singlet energy transfer and can lead to the generation of $^1O_2$ (Kellogg, 1969). The spontaneous or random collision of two $^1O_2$ can result in the dimol photon emission which is known to be emitted in the red region of the spectrum at the wavelengths of 634 nm and 703 nm or $^1O_2$ can alternatively undergo from singlet

excited state to ground triplet state accompanied by the monomol photon emission which is well known to be in the near IR region of the spectrum at the wavelengths of 1270 nm (Cadenas *et al*., 1980, Mathew and Roy, 1992, Pospíšil *et al*., 2014). Our results showing that ultra-weak photon emission was significantly decreased with the topical application of sodium ascorbate in Fenton's reagent-induced ultra-weak photon emission from porcine skin clearly shows that $^1O_2$ can contribute either directly through dimol emission or indirectly can be involved in the generation of LOOL (Fig. 21) to contribute to total ultra-weak photon emission. Similarly to this, two-dimensional Fenton's reagent-induced ultra-weak photon emission imaging results show considerable suppression under the effect of the presence of sodium ascorbate (Fig. 17, left panel). Our observation that ultra-weak photon emission under the effect of Fenton's reagent was enhanced in the near-infrared region of the spectrum and subsequently suppressed by the exogenous application of sodium ascorbate confirms the generation of $^1O_2$ during the oxidative radical reaction.

6 Conclusions

The current study presents the mechanism on the oxidation of polyunsaturated fatty acid which is one of the primary targets of ROS in the skin. It is aimed to understand the involvement of different electronically excited species ($^3L=O^*$ and $^1O_2$) in ultra-weak photon emission during the oxidative radical reactions. The results presented by means of ultra-weak photon emission kinetic measurement and two-dimensional imaging provides a series of evidence showing the contribution of these species in the overall ultra-weak photon emission. The methodology used to obtain the information/results clearly indicates that the ultra-weak photon emission can be used as a non-invasive tool without the involvement of any probes etc. The ultra-weak photon emission is thus claimed to serve as a potential tool for monitoring the physiological state of a biological system and can potentially be applied to different kinds of research areas such as dermatological research and/or clinical applications.

7 Funding

This work was financially supported by Student Grant Competition, grant No. IGA_PrF_2018_022 entitled "Modern Biophysics: New Directions and Perspectives".

8 References

Article citation:

ABDULLAHI, A., AMINI-NIK, S. & JESCHKE, M. G. 2014. Animal models in burn research. *Cellular and Molecular Life Sciences,* 71**,** 3241-3255.

ADAM, W. & CILENTO, G. 1982. *Chemical and biological generation of excited states,* New York, Academic Press.

AVON, S. L. & WOOD, R. E. 2005. Porcine skin as an in-vivo model for ageing of human bite marks. *The Journal of forensic odonto-stomatology,* 23**,** 30-9.

CADENAS, E., ARAD, I. D., BOVERIS, A., FISHER, A. B. & CHANCE, B. 1980. Partial Spectral-Analysis of the Hydroperoxide-Induced Chemi-Luminescence of the Perfused Lung. *Febs Letters,* 111**,** 413-418.

CADENAS, E. & SIES, H. 2000. Formation of electronically excited states during the oxidation of arachidonic acid by prostaglandin endoperoxide synthase. *Singlet Oxygen, Uv-a, and Ozone,* 319**,** 67-77.

CHARTIER, C., MOFID, Y., BASTARD, C., MIETTE, V., MARUANI, A., MACHET, L. & OSSANT, F. 2017. HIGH-RESOLUTION ELASTOGRAPHY FOR THIN-LAYER MECHANICAL CHARACTERIZATION: TOWARD SKIN INVESTIGATION. *Ultrasound in Medicine and Biology,* 43**,** 670-681.

CHIU, T. & BURD, A. 2005. "Xenograft" dressing in the treatment of burns. *Clinics in Dermatology,* 23**,** 419-423.

CIFRA, M. & POSPISIL, P. 2014. Ultra-weak photon emission from biological samples: Definition, mechanisms, properties, detection and applications. *Journal of Photochemistry and Photobiology B-Biology,* 139**,** 2-10.

CILENTO, G. & ADAM, W. 1995. FROM FREE-RADICALS TO ELECTRONICALLY EXCITED SPECIES. *Free Radical Biology and Medicine,* 19**,** 103-114.

COREY, E. J. & WANG, Z. 1994. Conversion of Arachidonic-Acid to the Prostaglandin Endoperoxide Pgg(2), a Chemical Analog of the Biosynthetic-Pathway. *Tetrahedron Letters,* 35**,** 539-542.

FOOTITT, S., PALLESCHI, S., FAZIO, E., PALOMBA, R., FINCH-SAVAGE, W. E. & SILVESTRONI, L. 2016. Ultraweak Photon Emission from the Seed Coat in Response to Temperature and HumidityA Potential Mechanism for Environmental Signal Transduction in the Soil Seed Bank. *Photochemistry and Photobiology,* 92**,** 678-687.

HALLIWELL, B. & GUTTERIDGE, J. 2007. *Free Radicals in Biology and Medicine, Ed 4,* Oxford, Oxford University Press.

HAVAUX, M. 2003. Spontaneous and thermoinduced photon emission: new methods to detect and quantify oxidative stress in plants. *Trends in Plant Science,* 8**,** 409-413.

HIKIMA, T., KANEDA, N., MATSUO, K. & TOJO, K. 2012. Prediction of Percutaneous Absorption in Human Using Three-Dimensional Human Cultured Epidermis LabCyte EPI-MODEL. *Biological & Pharmaceutical Bulletin,* 35**,** 362-368.

JACOBI, U., KAISER, M., TOLL, R., MANGELSDORF, S., AUDRING, H., OTBERG, N., STERRY, W. & LADEMANN, J. 2007. Porcine ear skin: an in vitro model for human skin. *Skin Research and Technology,* 13**,** 19-24.

JI, H. & LI, X.-K. 2016. Oxidative Stress in Atopic Dermatitis. *Oxidative Medicine and Cellular Longevity*.

KELLOGG, R. E. 1969. Mechanism of chemiluminescence from peroxy radicals. *Journal of the American Chemical Society,* 91**,** 5433-5436.

KOBAYASHI, M. 2005. *Two-dimensional imaging and spatiotemporal analysis of biophoton - Technique and applications for biomedical imaging*.

KONG, R. & BHARGAVA, R. 2011. Characterization of porcine skin as a model for human skin studies using infrared spectroscopic imaging. *Analyst,* 136**,** 2359-2366.

MADL, P., VERWANGER, T., GEPPERT, M. & SCHOLKMANN, F. 2017. Oscillations of ultra-weak photon emission from cancer and non-cancer cells stressed by culture medium change and TNF-alpha. *Scientific Reports,* 7.

MATHEW, B. G. & ROY, D. 1992. Weak luminescence from the frozen-thawed root tips of Cicer arietinum. L. *Journal of Photochemistry and Photobiology B-Biology,* 12**,** 141-150.

MEYER, W., NEURAND, K., SCHWARZ, R., BARTELS, T. & ALTHOFF, H. 1994. ARRANGEMENT OF ELASTIC FIBERS IN THE INTEGUMENT OF DOMESTICATED MAMMALS. *Scanning Microscopy,* 8**,** 375-391.

MEYER, W., SCHWARZ, R. & NEURAND, K. 1978. The skin of domestic mammals as a model for the human skin, with special reference to the domestic pig. *Current problems in dermatology,* 7**,** 39-52.

MIYAMOTO, S., MARTINEZ, G. R., MEDEIROS, M. H. G. & DI MASCIO, P. 2014. Singlet molecular oxygen generated by biological hydroperoxides. *Journal of photochemistry and photobiology B: Biology,* 139**,** 24-33.

MORRIS, G. M. & HOPEWELL, J. W. 1990. EPIDERMAL-CELL KINETICS OF THE PIG - A REVIEW. *Cell and Tissue Kinetics,* 23**,** 271-282.

MORROW, A. & LECHLER, T. 2015. Studying cell biology in the skin. *Molecular Biology of the Cell,* 26**,** 4183-4186.

NIGGLI, H. J., TUDISCO, S., LANZANO, L., APPLEGATE, L. A., SCORDINO, A. & MUSUMECI, F. 2008. Laser-Ultraviolet-A induced ultra weak photon emission in human skin cells: A biophotonic comparison between keratinocytes and fibroblasts. *Indian Journal of Experimental Biology,* 46**,** 358-363.

OU-YANG, H. 2014. The application of ultra-weak photon emission in dermatology. *Journal of Photochemistry and Photobiology B-Biology,* 139**,** 63-70.

POPLOVA, M., CERVINKOVA, K., PRUSA, J., PRASAD, A., POSPISIL, P., VAN WIJK, E. P. A. & CIFRA, M. 2017. Label-free chemiluminescence imaging of oxidative processes in human skin. *Free Radical Biology and Medicine,* 108**,** S63-S63.

POSPÍŠIL, P., PRASAD, A. & RÁC, M. 2014. Role of reactive oxygen species in ultra-weak photon emission in biological systems. *Journal of Photochemistry and Photobiology B-Biology,* 139**,** 11-23.

PRASAD, A., FERRETTI, U., SEDLÁŘOVÁ, M. & POSPÍŠIL, P. 2016. Singlet oxygen production in Chlamydomonas reinhardtii under heat stress. *Scientific Reports,* 6**,** 20094.

PRASAD, A. & POSPISIL, P. 2011a. Linoleic Acid-Induced Ultra-Weak Photon Emission from Chlamydomonas reinhardtii as a Tool for Monitoring of Lipid Peroxidation in the Cell Membranes. *Plos One,* 6**,** e22345.

PRASAD, A. & POSPISIL, P. 2011b. Two-dimensional imaging of spontaneous ultra-weak photon emission from the human skin: role of reactive oxygen species. *J Biophotonics,* 4**,** 840-9.

PRASAD, A. & POSPISIL, P. 2011c. Two-dimensional imaging of spontaneous ultra-weak photon emission from the human skin: role of reactive oxygen species. *Journal of Biophotonics,* 4**,** 840-849.

PRASAD, A. & POSPISIL, P. 2012. Ultraweak photon emission induced by visible light and ultraviolet A radiation via photoactivated skin chromophores: in vivo charge coupled device imaging. *Journal of Biomedical Optics,* 17**,** 085004.

PRASAD, A. & POSPISIL, P. 2013a. Towards the two-dimensional imaging of spontaneous ultra-weak photon emission from microbial, plant and animal cells. *Sci Rep,* 3**,** 1211.

PRASAD, A. & POSPISIL, P. 2013b. Towards the two-dimensional imaging of spontaneous ultra-weak photon emission from microbial, plant and animal cells. *Scientific Reports,* 3.

PROST-SQUARCIONI, C. 2006. Histology of skin and hair follicle. *M S-Medecine Sciences,* 22**,** 131-137.

RASTOGI, A. & POSPISIL, P. 2011. Spontaneous ultraweak photon emission imaging of oxidative metabolic processes in human skin: effect of molecular oxygen and antioxidant defense system. *Journal of Biomedical Optics,* 16**,** 096005.

RIFKIND, J. M., MOHANTY, J. G. & NAGABABU, E. 2015. The pathophysiology of extracellular hemoglobin associated with enhanced oxidative reactions. *Frontiers in Physiology,* 5.

RINNERTHALER, M., BISCHOF, J., STREUBEL, M. K., TROST, A. & RICHTER, K. 2015. Oxidative Stress in Aging Human Skin. *Biomolecules,* 5**,** 545-589.

RUSSELL, G. A. 1957. Deuterium-Isotope Effects in the Autoxidation of Aralkyl Hydrocarbons - Mechanism of the Interaction of Peroxy Radicals. *Journal of the American Chemical Society,* 79**,** 3871-3877.

SADRZADEH, S. M. H., GRAF, E., PANTER, S. S., HALLAWAY, P. E. & EATON, J. W. 1984. HEMOGLOBIN - A BIOLOGIC FENTON REAGENT. *Journal of Biological Chemistry,* 259**,** 4354-4356.

SAUERMANN, G., MEI, W. P., HOPPE, U. & STAB, F. 1999. Ultraweak photon emission of human skin in vivo: Influence of topically applied antioxidants on human skin. *Oxidants and Antioxidants, Pt B,* 300**,** 419-428.

TEPOLE, A. B., GOSAIN, A. K. & KUHL, E. 2012. Stretching skin: The physiological limit and beyond. *International Journal of Non-Linear Mechanics,* 47**,** 938-949.

TORINUKI, W. & MIURA, T. 1981. SINGLET OXYGEN AND ULTRAWEAK CHEMI-LUMINESCENCE IN RAT SKIN. *Tohoku Journal of Experimental Medicine,* 135**,** 387-393.

ZOUBOULIS, C. C. 2009. The skin as an endocrine organ. *Dermato-endocrinology,* 1**,** 250-2.

9 List of abbreviations

$^1O_2$	Singlet oxygen
$^3L=O^*$	Triplet excited carbonyls
CCD	Charged couple device
EPR	Electron paramagnetic resonance
$FeSO_4$	Iron sulfate
H_2O_2	Hydrogen peroxide
$HO^{\bullet}$	Hydroxyl radical
IR	Infrared radiation
L	Lipid molecule
$L^{\bullet}$	Alkyl radical
$LO^{\bullet}$	Lipid alcoxyl
$LOO^{\bullet}$	Lipid peroxyl radical
LOOH	Lipid hydroperoxide
LOOL	Dioxetane
LOOOOL	Tetroxide
PMT	Photomultiplier tube
POBN	4-pyridyl-1-oxide-N-tert-butylnitrone
ROI	Region of interest
ROS	Reactive oxygen species
UPE	Ultra-weak photon emission
UVA	Ultraviolet A

10 Appendices

- Title page of article submitted to journal (Frontiers in Physiology) based on part of results presented in the thesis.

Triplet excited carbonyls and singlet oxygen formation during oxidative radical reaction in skin

Ankush Prasad[1*], Anastasiia Balukova[1], Pavel Pospíšil[1]

[1]Department of Biophysics, Palacký University, Olomouc, Czechia

Submitted to Journal:
Frontiers in Physiology

Specialty Section:
Oxidant Physiology

Article type:
Original Research Article

Manuscript ID:
385572

Received on:
13 Apr 2018

Frontiers website link:
www.frontiersin.org